Biological Psychiatry: CNNI

Archival Report

A miR-137–Related Biological Pathway of Risk for Schizophrenia Is Associated With Human Brain Emotion Processing

Giulio Pergola, Antonio Rampino, Leonardo Sportelli, Christopher James Borcuk, Roberta Passiatore, Pasquale Di Carlo, Aleksandra Marakhovskaia, Leonardo Fazio, Nicola Amoroso, Mariana Nair Castro, Enrico Domenici, Massimo Gennarelli, Jivan Khlghatyan, Gianluca Christos Kikidis, Annalisa Lella, Chiara Magri, Alfonso Monaco, Marco Papalino, Madhur Parihar, Teresa Popolizio, Tiziana Quarto, Raffaella Romano, Silvia Torretta, Paolo Valsecchi, Hailiqiguli Zunuer, Giuseppe Blasi, Juergen Dukart, Jean Martin Beaulieu, and Alessandro Bertolino

ABSTRACT

BACKGROUND: miR-137 is a microRNA involved in brain development, regulating neurogenesis and neuronal maturation. Genome-wide association studies have implicated miR-137 in schizophrenia risk but do not explain its involvement in brain function and underlying biology. Polygenic risk for schizophrenia mediated by miR-137 targets is associated with working memory, although other evidence points to emotion processing. We characterized the functional brain correlates of miR-137 target genes associated with schizophrenia while disentangling previously reported associations of miR-137 targets with working memory and emotion processing.

METHODS: Using RNA sequencing data from postmortem prefrontal cortex (N = 522), we identified a coexpression gene set enriched for miR-137 targets and schizophrenia risk genes. We validated the relationship of this set to miR-137 in vitro by manipulating miR-137 expression in neuroblastoma cells. We translated this gene set into polygenic scores of coexpression prediction and associated them with functional magnetic resonance imaging activation in healthy volunteers (n_1 = 214; n_2 = 136; n_3 = 2075; n_4 = 1800) and with short-term treatment response in patients with schizophrenia (N = 427).

RESULTS: In 4652 human participants, we found that 1) schizophrenia risk genes were coexpressed in a biologically validated set enriched for miR-137 targets; 2) increased expression of miR-137 target risk genes was mediated by low prefrontal miR-137 expression; 3) alleles that predict greater gene set coexpression were associated with greater prefrontal activation during emotion processing in 3 independent healthy cohorts (n_1, n_2, n_3) in interaction with age (n_4); and 4) these alleles predicted less improvement in negative symptoms following antipsychotic treatment in patients with schizophrenia.

CONCLUSIONS: The functional translation of miR-137 target gene expression linked with schizophrenia involves the neural substrates of emotion processing.

https://doi.org/10.1016/j.bpsc.2023.11.001

Polygenic risk for schizophrenia (SCZ) is likely enacted via molecular pathways that affect neurophysiological phenotypes (1–3). The latest rendering of an SCZ genome-wide association study (GWAS) by the Psychiatric Genomics Consortium (PGC) has established a link with synaptic biology that is thought to be the basis of neural activity anomalies observed in individuals at genetic risk for SCZ (4,5). Accordingly, polygenic risk scores (PRSs) are associated with neural activity during working memory (WM) (6–9) and emotion processing (9–11), which are critical SCZ phenotypes. However, PRSs do not provide information about the molecular pathways that underlie the association of SCZ variants with system-level phenotypes because they collect signals from all biological pathways involved.

One strategy to integrate score computation with biological information is to study the targetomes of genetic regulators (3). MicroRNAs that target SCZ risk genes may be considered candidate master regulators involved in pathways relevant to SCZ risk (12). Of these microRNAs, miR-137 is among the most biologically plausible, exhibiting the most significant association with SCZ in GWASs (4,13) and SCZ clinical measures (14). The SCZ risk allele rs1625579, a miR-137 single nucleotide polymorphism (SNP), is associated with lower miR-137 expression in the dorsolateral prefrontal cortex (PFC) (15) and

with WM-related prefrontal activity. Two separate studies have also linked rs1625579 to an altered amygdala-prefrontal brain network during executive function and emotion processing tasks (16,17). This circuit has been consistently linked to emotion processing irrespective of miR-137 (18,19). Erk *et al.* (11) found that rs1702294, another miR-137 SNP, was associated with amygdala activity during emotion processing (11). These findings suggest that miR-137 may have a role in SCZ-related brain functional alterations during WM and emotion processing.

To link miR-137 to the biology of SCZ risk, Cosgrove *et al.* (20) parsed the SCZ PRS by including only miR-137 targets and found associations with brain activity during WM but not during emotion processing. While Erk *et al.* (11) found an association between the miR-137 mapping rs1702294 and emotion processing, their general SCZ PRS was differentially associated with episodic memory and social cognition. Polygenic approaches such as SCZ PRSs (11) may have diluted the effect of risk pathways that affect emotion processing with unrelated signals even when parsed for miR-137 targets (20), e.g., because only a subset of the SCZ loci targeted by miR-137 is associated with emotion processing or because PRSs do not reflect specific biological processes. An alternative method to capture the implication of miR-137 genetic variation on functional brain phenotypes previously associated with SCZ risk is to use gene coexpression (3).

Here, we investigated 1) coexpression of miR-137 target genes in the human PFC and their relationship with SCZ risk; 2) association of genetic variants in miR-137 target coexpression pathways with WM or emotional face recognition brain activity in humans; and 3) their association with symptom improvement in patients with SCZ after short-term treatment with antipsychotics. In parallel, we assessed these same associations considering all miR-137 targets regardless of coexpression to investigate whether coexpression-defined targets would increase the precision of prediction. Figure 1 illustrates a synopsis of the study.

We generated 2 genetic scores to study miR-137 target gene variation. A polygenic coexpression index ($PCI_{miR-137}$) (21–23) indexed the predicted expression of a subset of miR-137 targets associated with SCZ risk that are coexpressed in the PFC. Therefore, this index identifies a miR-137–related

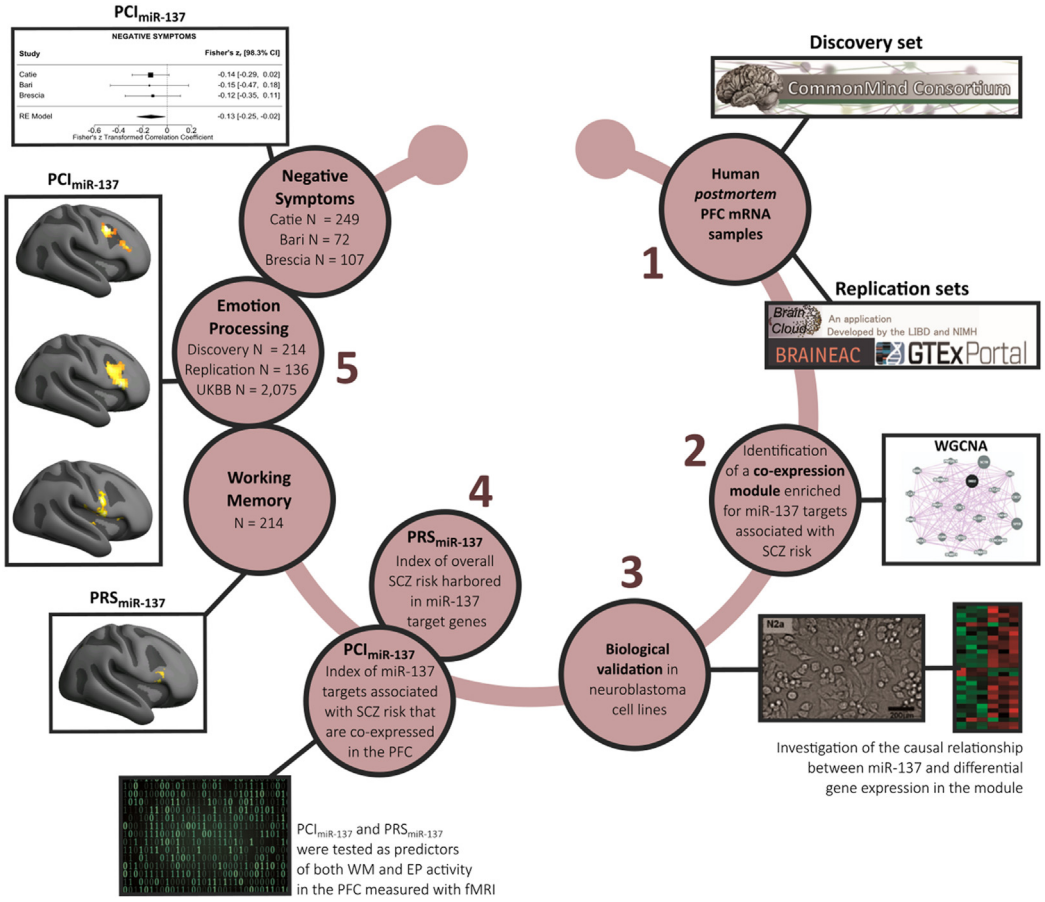

Figure 1. Study design. The figure illustrates the multistep procedure that was used to translate postmortem brain gene expression into predictions of prefrontal activity during task performance in fMRI. EP, emotion processing; fMRI, functional magnetic resonance imaging; GTEx, Genotype-Tissue Expression; LIBD, Lieber Institute for Brain Development; mRNA, messenger RNA; NIMH, National Institute of Mental Health; PCI, polygenic coexpression index; PFC, prefrontal cortex; PRS, polygenic risk score; RE, random effect; SCZ, schizophrenia; UKBB, UK Biobank; WGCNA, weighted gene coexpression network analysis; WM, working memory.

biological pathway of risk, but not necessarily participant-level risk, for SCZ. A $PRS_{miR\text{-}137}$ included the overall statistical risk for SCZ harbored in miR-137 target genes weighted by their GWAS-derived effect size (20). This score is an index of miR-137–related participant-level genetic risk for SCZ. Both $PCI_{miR\text{-}137}$ and $PRS_{miR\text{-}137}$ were tested as predictors of functional magnetic resonance imaging (fMRI) WM/emotional face recognition activation in the PFC and symptom improvement after antipsychotic treatment in patients with SCZ.

METHODS AND MATERIALS

Experimental Design

Identification of a Gene Coexpression Network in the Human PFC. CommonMind Consortium RNA sequencing data from postmortem PFC (24) served to identify a gene coexpression network in neurotypical individuals using weighted gene coexpression network analysis (WGCNA) (25). A dataset matching the fMRI sample on age and ancestry included 147 neurotypical Caucasian adults (demographics in Table S1 in Supplement 1; Section 1.1 in Supplement 1). After correcting the expression data for confounding variables, such as the linear and quadratic effects of RNA integrity number, postmortem brain tissue pH, age, postmortem interval, institute, sex, and library batch, we computed a WGCNA as previously reported (22) on 17,173 genes (Section 1.1 in Supplement 1).

We validated the discovered gene-gene relationships using 3 independent datasets [BrainEAC (Brain eQTL Almanac) frontal cortex (n = 123) (26), Braincloud PFC Brodmann area (BA) 46 (n = 59) (27), and Genotype-Tissue Expression (GTEx) (28) PFC BA 9 (n = 183)] (Table S1 in Supplement 1; Section 1.1 in Supplement 1) (29) and assessed the replication of each coexpressed gene set, called a module, using preservation (30) and permutation techniques (Section 1.1 in Supplement 1). Briefly, for each discovery module and replication dataset, we computed the median of its topological overlap matrix and compared this value against the null distribution of medians computed on 10,000 random modules of identical size. We calculated the replication p values for each module through a meta-analytic approach summarizing the p values obtained (sum-log Fisher's method; $\alpha_{Bonferroni} = 0.05/[N_{modules} \times 3]$). We also assessed the replication of the discovered coexpression patterns in the GTEx amygdala dataset (n = 127) (Table S1 in Supplement 1) as previously described.

Module Prioritization and Functional Analysis. We assessed the overlap between genes in the replicated coexpression modules and miR-137 target genes derived via a meta-analysis of 4 microRNA target databases (31–34) (sum-log Fisher's method; $\alpha_{Bonferroni} = 0.05/[\text{replicated } N_{modules}]$). Then, we assessed the overrepresentation of 120 genes prioritized by the latest PGC3 GWAS (4) within the miR-137–enriched modules (Table S2 in Supplement 2; Section 1.2 in Supplement 1).

We investigated module function via enrichments for cell-type markers (35), transcriptome-wide associations (36–38), gene ontologies (PANTHER) (39), chromosomal locus (40), and brain region-specific expression during neurodevelopment (41) (Section 1.2 in Supplement 1). To validate the association of coexpressed genes within each module with SCZ genetic risk or miR-137, we computed the correlation between the module eigengene and the PGC3 SCZ PRS (4) or $PRS_{miR\text{-}137}$ (20) (described below), respectively.

Experimental Validation in Neuroblastoma Cells and Data Analysis. We directly assessed the contribution of miR-137 to the regulation of prioritized modules by a cell model allowing for titration of miR-137 expression. Using Neuro2A neuroblastoma cells, miR-137 was either overexpressed through PcDNA3.2/V5 mmu-mir-137 plasmid transfections or knocked down through a CRISPR-Cas9 approach (42) (Figure S5 in Supplement 1). The impact of dose-dependent linear changes in miR-137 expression on transcriptome-wide expression was evaluated using microarrays (Mouse Gene 2.0 ST microarrays, Afymetrix/Thermo Fisher) (Section 1.4 in Supplement 1). In the linear models, gene expression was the dependent variable, and miR-137 quantification was the predictor. We assessed overrepresentation of dose dependently expressed genes (DDEGs) (false discovery rate–corrected $q < .05$) in the target modules (Section 1.4 in Supplement 1) and of SCZ risk genes among the DDEGs (hypergeometric test). We assessed the overrepresentation of genes differentially regulated in rodents following genetic knockout (43) and overexpression (44) of miR-137 in all replicated modules.

Expression Imputation of miR-137 Target Genes: SNP Identification. The $PCI_{miR\text{-}137}$ was computed to test system-level phenotypes associated with the module of interest. We identified SNPs in the module genes associated with the first principal component of module gene expression (a measure of coexpression of the module) (21,23,27,45–49) (Section 1.5 in Supplement 1), estimated the effect of allelic dosage via a robust linear model (rlm function—robust R package), and ranked SNPs according to their p values (22). We assessed the top 50 ranked SNPs (22) and picked the top SNPs that replicated the association with coexpression in the largest replication dataset that we had available (BrainEAC) (Section 1.5 in Supplement 1).

Neuroimaging Study

University of Bari Aldo Moro Sample. We recruited 350 healthy volunteers distributed in a discovery cohort of 214 participants with both emotional face recognition and WM data and a replication cohort of 136 participants for the emotional face recognition task only (Table S1 in Supplement 1). Inclusion/exclusion criteria have been described elsewhere (Section 1.6 in Supplement 1) (50). Participants signed an informed consent form complying with the Declaration of Helsinki after fully explaining all procedures approved by the local ethics committee.

UK Biobank Sample. This cohort included older participants than the University of Bari Aldo Moro (UNIBA) cohorts (Table S1 in Supplement 1); therefore, we split the UK Biobank sample by median age (58 years) into 2 subsamples of 2075 and 1800 healthy individuals, respectively, so that the younger

UK Biobank subsample matched the upper age limit of the UNIBA discovery sample [see Section 1.6 in Supplement 1 and http://www.ukbiobank.ac.uk/ (51)]. The UK Biobank received regular ethical approval (reference 11/NW/0382). All participants provided informed consent (http://biobank.ctsu.ox.ac.uk/crystal/field.cgi?id=200). All participants included in this study are of European ancestry (Section 1.6 in Supplement 1; Figures S8, S9 in Supplement 1).

Genetic Score Computation. We genotyped all participants (52) and performed imputation and quality checks (Section 1.6 in Supplement 1) [see (53) for UK Biobank]. The $PCI_{miR\text{-}137}$ is the average of coexpression effects of the selected SNP alleles in the postmortem study, which were replicated in the BrainEAC. A subset of the selected SNPs was used to calculate the $PCI_{miR\text{-}137}$ in the UK Biobank sample due to array differences or quality control procedures (see Results and Section 1.6 in Supplement 1 for additional details). Instead, we computed the $PRS_{miR\text{-}137}$ for SCZ using standard procedures (54) with the miR-137 target gene list and SNPs previously reported (20) (the SNP-level significance thresholds were $p < 10^{-5}$, $p < .05$, and $p < .5$). Notably, previously reported scores relied on PGC2 GWAS statistics (13). Here, in addition to replicating Cosgrove *et al.*'s findings (20), we tested the most recent [PGC3 (4)] PRSs computed with their same method (20). Scores computed to control for possible confounders are reported in Sections 1.5, 1.7, and Supplemental Results in Supplement 1.

Experimental Procedures. Emotional face recognition ("Faces") and WM ("N-Back") tasks were acquired at UNIBA (55–60), whereas the Faces Matching Task (61,62) was used in the UK Biobank (Section 1.6 in Supplement 1). fMRI data collection, preprocessing, and analysis followed standard procedures (Section 1.5 in Supplement 1) (27,63).

Statistical Analysis. We used SPM12 to perform the analyses. For the coexpression analysis, we used the linear and quadratic terms of $PCI_{miR\text{-}137}$ (21,45,49) as predictors and age, sex, and 5 genomic eigenvariates as covariates in a multiple regression model. For the $PRS_{miR\text{-}137}$ analyses, we used PRSs as predictors and the same covariates reported above. For the UNIBA WM/Faces discovery sample, we report results thresholded at the whole-brain level masked by task activity at peak or cluster level, adjusted for multiple comparisons as the number of voxels (familywise error–corrected p [p_{FWE}] $< .05$). In the UNIBA Faces replication sample, we obtained a more inclusive mask of the cluster detected in the discovery analysis thresholded at voxelwise $p < .05$ uncorrected and performed a small-volume correction ($p_{SVC} < .05$). Because the UK Biobank dataset differed in terms of age distribution, experimental procedure, and $PCI_{miR\text{-}137}$ computation, we first tested the effect of $PCI_{miR\text{-}137}$ on the whole sample through analysis of covariance including the age group × $PCI_{miR\text{-}137}$ interaction to account for possible aging effects. Then, multiple regression models were independently computed in both UK Biobank subsamples to validate the results obtained in the UNIBA sample including the age × $PCI_{miR\text{-}137}$ interaction. We thresholded the results at $p < .05$ at the whole-brain level masked by task activity at peak or cluster level ($p_{FWE} < .05$), followed by small-volume correction ($p_{SVC} < .05$) to verify the overlap with the significant voxels from the UNIBA sample discovery analysis.

A connectivity analysis linked miR-137 target gene–predicted expression in the dorsolateral PFC with prefrontal-amygdala functional coupling using a genetic-physiological interaction approach (64). Here, we used the prefrontal seed associated with the $PCI_{miR\text{-}137}$ and extracted movement- and task-corrected estimates from the bilateral amygdala [Wake Forest University Pickatlas (17)] (Section 1.6 in Supplement 1).

Clinical Study

We assessed the clinical relevance of the $PRS_{miR\text{-}137}$ and $PCI_{miR\text{-}137}$ by testing their associations with clinical readouts in patients with SCZ (Table S1 in Supplement 1; Section 1.7 in Supplement 1). We included 3 independent clinical cohorts, from the CATIE (Clinical Antipsychotic Trials of Intervention Effectiveness) Project (65), UNIBA, and the University of Brescia. Cohorts were evaluated at baseline and after either 2 weeks or 1 month of treatment, as described in Section 1.8 in Supplement 1. We assessed symptom improvement rated with the Positive and Negative Syndrome Scale and calculated as 100 × (baseline − end point)/baseline evaluations, using the sum of the positive, negative, and general Positive and Negative Syndrome Scale items, so that a higher score indicates higher improvement. To investigate the association between $PRS_{miR\text{-}137}$ and $PCI_{miR\text{-}137}$ and positive and negative symptoms, we generated a linear model with symptom improvement in each domain as the dependent variable and age, sex, and the first 10 genomic eigenvariates as covariates. We performed a meta-analysis of Fisher's z-transformed correlation coefficients obtained using a random-effects mixed model (rma.uni function of the metafor R package, https://cran.r-project.org/web/packages/metafor/metafor.pdf). Bonferroni correction was used to adjust for multiple comparisons.

RESULTS

miR-137 Targets and SCZ Risk Genes Were Coexpressed in the "Darkorange" Module

Our gene coexpression network included 51 modules plus the gray module of 3018 nonclustered genes. Permutation tests revealed that gene-gene relationships in 35 of 51 modules were preserved in 3 replication datasets (Bonferroni-adjusted $p < \alpha_{Bonferroni} = 0.05/[50] = .00098$) (Figure S1 in Supplement 1). Gene loadings on the module expression were concordant across replication datasets (binomial p values, all $p < 10^{-12}$) (Figure S2 in Supplement 1), suggesting reproducible directions of gene-gene relationships. These gene-gene relationships were largely replicated in the amygdala (Figure 2A). Next, enrichment for miR-137 targets was evaluated for each module, drawing from a universe of 1935 miR-137 target genes derived from 4 bioinformatic tools (Section 1.2 in Supplement 1). We found 6 of the 35 reproducible modules enriched for miR-137 target genes (Bonferroni-adjusted $p < \alpha_{Bonferroni} = 0.05/[35] = .0014$) (Table S3 in Supplement 2; Figure 2A). Of these 6 modules, only darkorange (173 genes) (Table S4 in Supplement 2) was significantly

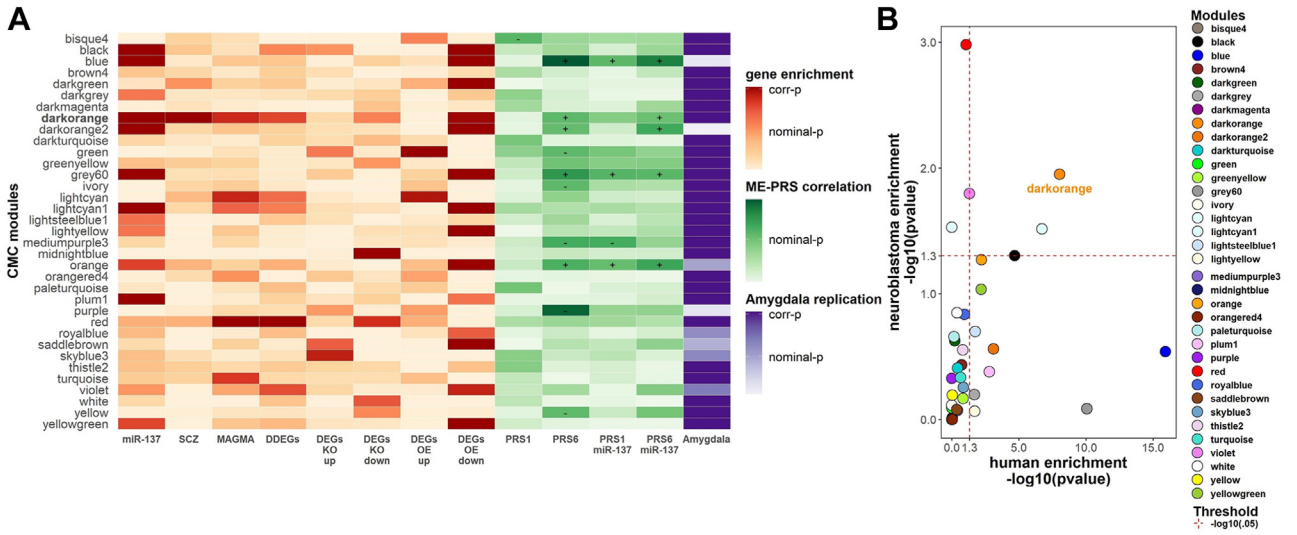

Figure 2. Module prioritization. **(A)** Overview of the overrepresentation in all replicated modules (35 of 51). Each column in the heatmap shows a color-coded association probability between the module and the variable. Gene enrichment analyses (red palette) represent hypergeometric tests of overrepresentation of gene lists; module eigengene-PRS associations (green palette) represent the *p* value of Pearson's correlations; amygdala replication (violet palette) represents the empirical probability of gene-gene correlations within a module using a null distribution. Individual columns illustrate miR-137: miR-137–predicted targets in humans (meta-analysis of 4 target prediction databases); SCZ: PGC3 SCZ genes (42); MAGMA: PGC3 genetic variants associated with SCZ (MAGMA, competitive enrichment analysis); DDEGs: DDEGs in neuroblastoma cells (list derived from false discovery rate–corrected $q < .05$ linear covariation with miR-137 concentration); DEGs KO/OE up/down: DEGs in 2 murine models (44,45) divided into upregulated and downregulated genes; PRS 1/PRS 6: association of module eigengenes with PRS for SCZ at genome-wide (PRS 1: $p = 5 \times 10^{-8}$) or nominal (PRS 6: $p = .05$) single nucleotide polymorphism inclusion significance (+ indicates a positive nominally significant correlation, and − indicates a negative nominally significant correlation); PRS 1/PRS 6 miR-137, association with the $PRS_{miR-137}$; amygdala, replication empirical *p* value in the amygdala. The colormap highlights darkorange relative to other modules. **(B)** Scatterplot illustrates the enrichment of each replicated module for miR-137 targets as assessed in neuroblastoma cells and in bioinformatic predictions in humans. The 2 assessments covaried except for the blue and red outliers. CMC, CommonMind Consortium; DDEG, dose dependently expressed gene; DEG, differentially expressed gene; KO, knockout; ME, module eigengene; OE, overexpressed; PGC, Psychiatric Genomics Consortium; PRS, polygenic risk score; SCZ, schizophrenia.

enriched for genes in the SCZ risk loci (Bonferroni-adjusted $p = 8.910^{-5} \times 6 = .0005$) (Figure 2A, column 2); 7 of 156 protein-coding genes in 7 risk loci (Table S8 in Supplement 2) and 101 of 120 SCZ genes (4) were annotated in the network; 14,939 protein-coding genes were represented the enrichment background. Darkorange genes were also associated with greater SCZ risk than other replicated modules using MAGMA (66) (Bonferroni-adjusted $p = .0012 \times 35 = .042$) (Figure 2A). The first principal component of darkorange gene expression explained 54% of *Darkorange* expression variance and was positively correlated with the PGC3-PRS6 for SCZ in the CommonMind Consortium cohort ($n = 147$, $t_{146} = 2.11$, $p = .036$) (Figure 2A). Six of 7 SCZ risk darkorange genes were also predicted miR-137 targets, encompassing 19.4% (6 of 31) of genes in the network that were both PGC3 hits and predicted miR-137 targets (Figure 3A). We validated the relationship between darkorange, SCZ risk, and miR-137 target genes (Section 1.3 and Supplemental Results in Supplement 1), and through permutation analysis, we determined that this 3-way interaction was highly significant (Section 1.3 in Supplement 1) (empirical $p < .0001$).

Darkorange Was Enriched for Neuronal Markers and Gene Ontologies Relevant to Neuronal Function

The cell-type marker overrepresentation analysis ascribed the darkorange module to excitatory and inhibitory neurons (excitatory PFC: Bonferroni-adjusted $p = 4.7 \times 10^{-19} \times 35 \times 10 = 1.6 \times 10^{-16}$; GABAergic [gamma-aminobutyric acidergic] neurons: Bonferroni-adjusted $p = 4.4 \times 10^{-15} \times 35 \times 10 = 1.5 \times 10^{-12}$) (Figure S3 in Supplement 1), and the specific expression analysis across brain regions and development revealed that darkorange genes were preferentially expressed in the PFC during young adulthood ($p_{corrected} = 1.7 \times 10^{-5}$ [specificity index probability $< .01$]) (Figure S4 in Supplement 1). Accordingly, the darkorange module was functionally enriched for synaptic signaling (GO:0099536, 19 genes, fold enrichment = 5.8, $p_{corrected} = 8.4 \times 10^{-6}$) and nervous system development (GO:0007399, 41 genes, fold enrichment = 2.4, $p_{corrected} = 6.4 \times 10^{-4}$) (Figure 3B). This evidence suggests that the miR-137–related coexpression patterns found in this module are more closely associated with prefrontal neuronal functioning and maturation than glia during adolescence, a crucial developmental period for the onset of SCZ psychopathology (67,68). No significant results were found for transcriptome-wide associations or chromosome locus overrepresentation analyses ($p > .05$).

Darkorange Was Enriched for Genes Modulated by miR-137

Evaluation of miR-137 expression using quantitative polymerase chain reaction confirmed the efficacy of the knockdown and overexpression procedures (Table S5 in Supplement 1).

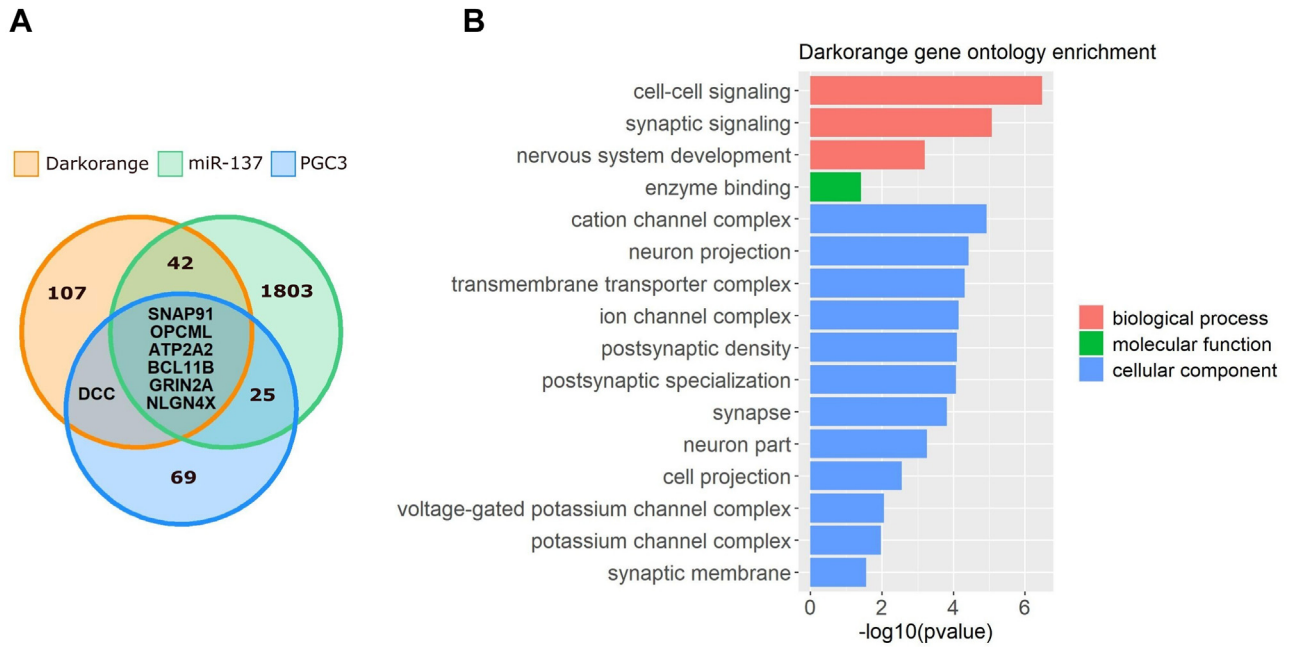

Figure 3. Darkorange module features. **(A)** Intersection between darkorange genes, PGC3 schizophrenia genes, and miR-137 targetome bioinformatic predictions in humans. **(B)** Gene ontologies associated with darkorange genes. Reported *p* values are corrected for multiple comparisons. PGC, Psychiatric Genomics Consortium.

We identified 580 DDEGs that showed linear covariation with miR-137 (false discovery rate–corrected $q < .05$). The DDEG set was also enriched for miR-137–predicted targets (hypergeometric test, $p = 1.27 \times 10^{-77}$). Except for 2 outlier modules [red and blue, over 3 standard deviations from the mean over-representation expressed as $-\log_{10}(p)$], there was good agreement between module enrichment for bioinformatically predicted miR-137 targets and module enrichment for DDEGs (Figure 2A), as shown by a significant positive correlation across modules ($n = 33$ after outlier removal, $r = 0.41$, $p = .017$). The darkorange module included 13 DDEGs of 141 genes expressed in neuroblastoma cells, which is a significant proportion ($p = .011$) (Figure 2B; Figure S6 in Supplement 1). Moreover, the darkorange module was enriched for genes independently associated with miR-137 knockout (43) ($p = .041$) (Figure 2A) and overexpression (44) ($p = .0017$) (Figure 2A). Only a few modules overrepresented miR-137 DDEGs (Figure 2A), supporting the relative specificity of the darkorange module for miR-137 targets.

The PCI Combined Reproducible Associations of SNPs With Darkorange

Fifteen of the SNPs in the darkorange genes were associated with the first principal component of darkorange gene expression. PCIs including 7 to 15 of the most darkorange-associated SNPs were replicated (BrainEAC: 1-tailed $p < .05$). Table S9 in Supplement 2 includes annotations of the 15 SNPs; Table S6 in Supplement 1 reports allelic weights. The $PCI_{miR\text{-}137}$ including 15 SNPs was tested in the UNIBA neuroimaging samples, while a subset of 9 SNPs formed the $PCI_{miR\text{-}137}$ that was tested in the UK Biobank sample (Section 1.5 and Section 1.7 in Supplement 1).

Neuroimaging Revealed an Association of miR-137–Related Coexpression With Emotion Processing

Complete fMRI statistics are reported in Table S7 in Supplement 1. During the Faces task, the linear term of the $PCI_{miR\text{-}137}$ was positively correlated with activation in a right prefrontal cluster, including BA 8, 9, and 46, in the discovery sample (peak Z = 4.7; $p_{FWE} = .004$; 57 voxels; Montreal Neurological Institute [MNI] coordinates x = 50, y = 12, z = 42, $R^2 = 0.1$) (Figure 4A). We replicated the effect in the replication sample (peak Z = 3.7, $p_{SVC} = .007$; 34 voxels; MNI coordinates x = 50, y = 19, z = 31, $R^2 = 0.1$) (Figure 4B). Therefore, greater darkorange-predicted coexpression was associated with lower miR-137 expression (see Figure S6 in Supplement 1) and greater prefrontal activity during emotion processing. Greater $PCI_{miR\text{-}137}$ was also associated with lower prefrontal-amygdala connectivity during emotion processing ($p_{SVC} < .05$) (Figure S7 in Supplement 1). We found no effect of $PRS_{miR\text{-}137}$ on the Faces task. We found no effect from PCIs derived from the 5 modules that were associated with miR-137 but not with SCZ.

In the whole UK Biobank sample, we found no significant main effect of $PCI_{miR\text{-}137}$ in the context of a significant age group $\times$ $PCI_{miR-137}$ interaction during the Faces Matching Task overlapping the cluster detected in the discovery sample (peak Z = 3.79, $p_{SVC} = .015$; 84 voxels; MNI coordinates x = 50, y = 24, z = 40, $R^2 = 0.004$) (Figure S10B, C in Supplement 1) such that the effect of the $PCI_{miR\text{-}137}$ on blood oxygen level–dependent signal estimated during emotion processing was in the opposite direction as a function of the age stage. In the younger UK Biobank subsample, a $PCI_{miR\text{-}137}$ showed a positive linear association with right prefrontal activation in a cluster encompassing BA 44, BA 46, and BA 45 at 12 mm from the discovery cluster (peak Z = 3.72; cluster-level $p_{FWE} = .04$;

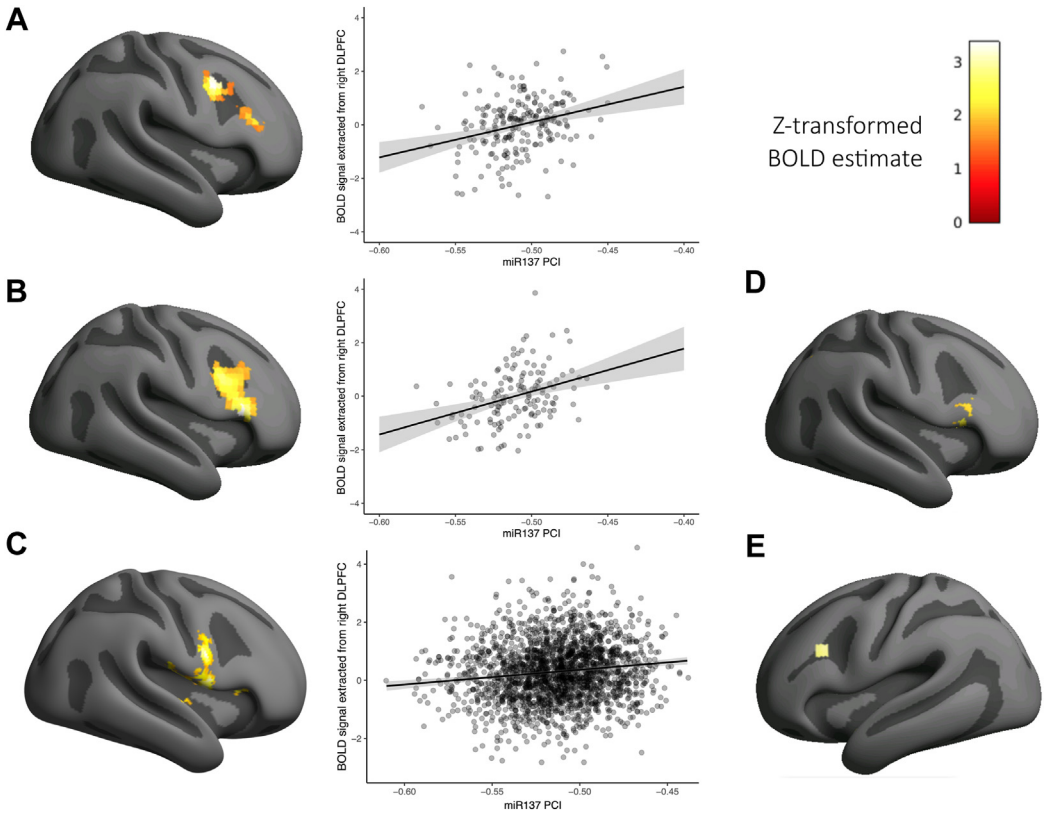

Figure 4. Association of miR-137–related coexpression with emotion processing and working memory. **(A–C)** Rendering of the brain activation positively associated with $PCI_{miR\text{-}137}$ during emotion processing in the **(A)** University of Bari Aldo Moro discovery, **(B)** replication, and **(C)** UK Biobank samples. **(D, E)** Rendering of the brain activation **(D)** during working memory associated with a PGC2-derived $PRS_{miR\text{-}137}$ and **(E)** with the complementary score computed using PGC3-schizophrenia variants not harbored within miR-137. Color bar indicates *z* scores. Right in the figures is right in the brain. Each scatterplot refers to the cluster highlighted in the rendering on its top. In the scatterplots, axes are scaled with mean = 0 and SD = 1. BOLD, blood oxygen level–dependent; DLPFC, dorsolateral prefrontal cortex; PCI, polygenic coexpression index; PGC, Psychiatric Genomics Consortium; PRS, polygenic risk score.

k = 1685; MNI coordinates x = 38, y = 28, z = 10, R^2 = 0.01) (Figure 4C; Section 1.7 and Supplemental Results in Supplement 1). This cluster overlapped by 10 voxels with the discovery cluster (peak Z = 2.09; $p_{uncorrected}$ = .018; p_{SVC} = .6; MNI coordinates x = 54, y = 8, z = 34, R^2 = 0.001). In the older UK Biobank subsample, we found no significant main effect of $PCI_{miR\text{-}137}$ in the context of a significant age × $PCI_{miR-137}$ interaction overlapping with the cluster detected in the discovery sample (peak Z = 3.58; p_{SVC} = .031; 154 voxels; MNI coordinates x = 50, y = 22, z = 38, R^2 = 0.007) (Figure S10A in Supplement 1).

We found no significant effect of the $PCI_{miR\text{-}137}$ on WM-related activity, in contrast to the independently reported association of WM-related activity with a PGC2 derived $PRS_{miR\text{-}137}$ by Cosgrove *et al.* (20). Replicating their result, we found that a PGC2-derived $PRS_{miR\text{-}137}$ was positively correlated with WM activity in the frontoparietal network, including a right prefrontal cluster spanning the anterior cingulate cortex and BA 9/8/44 (peak Z = 4.0; peak p_{FWE} = .061; cluster-level p_{FWE} = .036; 76 voxels; MNI coordinates x = 8, y = 23, z = 28/ x = 27, y = 30, z = 35/ x = 42, y = 16, z = 31) (Figure 4D). This effect was not observed when using SCZ risk variants not harbored within miR-137 targets (Figure S7 in Supplement 1). When we tested a PGC3-derived $PRS_{miR\text{-}137}$, results for WM were no longer significant. Instead, the complementary score computed using SCZ variants not harbored within miR-137 targets at the same threshold ($p < .5$) was associated with WM activity, with a significant cluster spanning BA 44/47 (peak Z = 4.1; peak p_{FWE} = .03; cluster-level p_{FWE} = .12; 40 voxels; MNI coordinates x = −40, y = 27, z = 9) (Figure 4E).

The Polygenic Index of miR-137–Related Coexpression Was Correlated With Negative Symptom Improvement in Patients With SCZ After Short-Term Treatment With Antipsychotics

Consistent with the association with brain activity during emotion processing, improvement in negative symptoms was negatively associated with the $PCI_{miR\text{-}137}$ (98.3% CI derived from $\alpha_{Bonferroni}$ = 0.05 × 3 = .017; *z*-transformed coefficient [98.3% CI]: −0.13 [−0.25 to −0.02]) (Figure 5). The $PRS_{miR\text{-}137}$ showed no significant association with symptoms. These results suggest that greater darkorange gene expression is associated with less improvement in negative symptoms after short-term antipsychotic treatment.

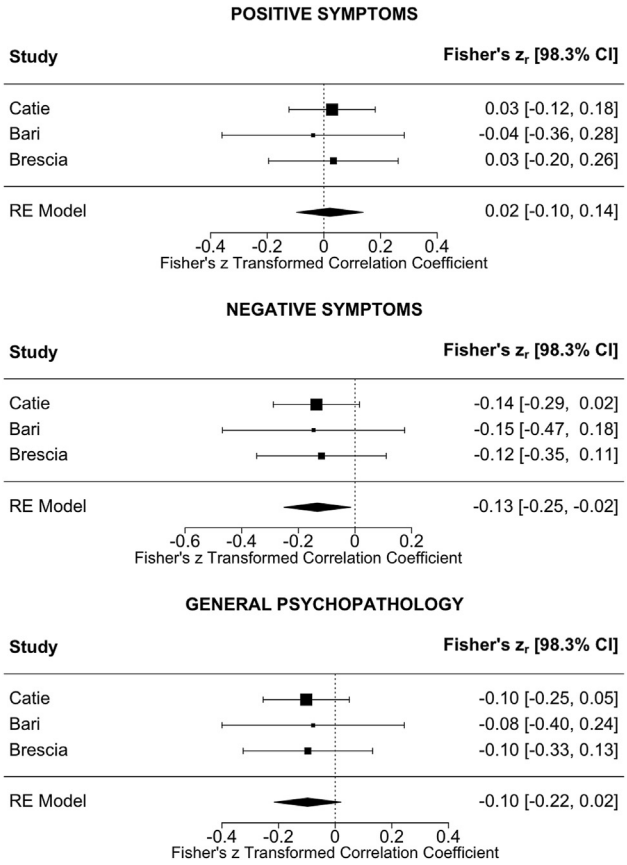

Figure 5. $PCI_{miR\text{-}137}$ association with schizophrenia symptom improvement. Forest plot for the meta-analytic association of positive, negative, and general symptom improvement with $PCI_{miR\text{-}137}$. Squares represent Fisher's *z*-transformed correlation coefficients obtained for each site with horizontal confidence interval bars ($1 - \alpha$, where α is corrected for comparison across 3 domains). Diamonds represent the RE model–derived meta-analytic linear coefficient with lateral tips showing confidence intervals. The dotted vertical line indicates no significant effect. Names of clinical cohorts are shown on the left; coefficients and confidence intervals are shown on the right. PCI, polygenic coexpression index; RE, random effect.

DISCUSSION

Emotion processing and WM have been proposed as core features in multiple brain disorders (69). However, the severity of emotion processing and WM impairments seems to be more pronounced in SCZ (70,71), and they have been proposed as SCZ intermediate phenotypes (72,73). Here, we sought to disentangle the effects of SCZ risk–related genetic pathways of miR-137 regulation on brain functional phenotypes associated with SCZ risk to shed light on the biological mechanisms underlying SCZ.

We hypothesized that miR-137 regulates coexpression of SCZ risk genes prioritized in the latest PGC3 GWAS in the human PFC and evaluated the involvement of miR-137 targets in WM and emotion processing. We identified a coexpression module (darkorange) that shows overrepresentation of SCZ genes and the regulation of which by miR-137 is supported by in vitro and in vivo experimental evidence. We validated the association of darkorange genes with miR-137 in a neuroblastoma cell model and 2 published datasets. We characterized the functional genetics of darkorange and developed an index of coexpression of genes in this module. *SNAP91*, *CACNB2*, *ATP2A2*, *BCL11B*, *GRIN2A*, and *NLGN4X* genes were at the intersection between miR-137–associated coexpression and SCZ risk. *ATP2A2* is one of the genes with the widest support for coexpression with other SCZ risk genes in the PFC (74). Darkorange genes have greater expression levels in neurotypical adults with greater SCZ genetic risk and in individuals with low miR-137 expression. Gene ontology analysis links darkorange genes with neurodevelopment and synaptic signaling. Coexpression of darkorange genes and miR-137 target gene SCZ risk reflected by $PCI_{miR\text{-}137}$ and $PRS_{miR\text{-}137}$, respectively, were associated with distinct neuroimaging readouts.

While replicating previous evidence that a PGC2-derived $PRS_{miR\text{-}137}$ is associated with prefrontal activity during WM, when including SCZ risk variants significant in the PGC3 SCZ GWAS, we found that the association with prefrontal activity was not specific to miR-137 target genes while being more generally linked with the SCZ PRS not including miR-137 targets. This result confirms Cosgrove *et al.*'s (20) findings, while showing that the link between SCZ genetic risk and WM goes beyond miR-137 targets. When considering genetic variation indexing miR-137–regulated gene coexpression in the same brain region by the $PCI_{miR\text{-}137}$, we discovered that the $PCI_{miR\text{-}137}$ was positively related to prefrontal activity but negatively related to prefrontal-amygdala coupling during emotion processing and unrelated to WM. Furthermore, greater $PCI_{miR\text{-}137}$ was associated with less improvement in negative but not positive or general symptoms in patients with SCZ, improving understanding of functional genomics involving miR-137 (3). Previous reports might be inconsistent about the functional role of miR-137 in brain imaging phenotypes because of the limits of GWAS-derived scores. Instead, coexpression effects are directional: Greater target gene expression is associated with lower miR-137 expression and higher SCZ risk.

Common Variation in Target Genes of miR-137 Was Related to Emotion Processing

In this study, we analyzed around 4600 individuals across the UNIBA and UK Biobank samples, which is larger than previously tested cohorts (17,20), the sizes of which ranged up to 86 participants. Because we assessed neurotypical individuals without a familial psychiatric history, findings indicate that greater miR-137 target gene expression (mostly associated with lower miR-137 expression, Figure S6 in Supplement 1)—in turn linked with greater SCZ risk (15)—is associated with greater prefrontal activity, possibly influenced by age effects and lower prefrontal-amygdala coupling during emotion processing. We speculate that lower miR-137 expression in the PFC is associated with risk for SCZ by increased target gene expression.

Limitations

Only 50 of the 1935 bioinformatically predicted miR-137 targets have been experimentally validated (75), although the number is likely to be higher. Because parsing 50 genes

across 51 coexpression modules would be inadequate for enrichment analysis, we relied on predictions, as has been done elsewhere (20). We endeavored to address this limitation through in vitro experiments showing that darkorange stands out at the intersection between bioinformatics and neuroblastoma cell findings (Figure 2B). Data from 2 in vivo models of miR-137 knockout and overexpression provided further support for the association between darkorange and miR-137. For the UK Biobank replication, we could only use 9 instead of 15 SNPs used for $PCI_{miR\text{-}137}$ computation in the UNIBA samples, which likely impacted our statistical effects (Section 1.5 in Supplement 1). It is also possible that the analysis in the smaller discovery and replication UNIBA samples yielded inflated effect sizes due to the higher variability typically associated with small sample sizes (76).

Conclusions

Genes coexpressed in darkorange overrepresented both SCZ risk genes and miR-137 targets, suggesting that miR-137–mediated coexpression may represent a point of convergence of genetic risk for SCZ. These genes were synergistically overexpressed in adults at greater risk for SCZ and individuals with lower PFC miR-137 expression from our postmortem investigation. Moreover, miR-137 SCZ-related coexpression was correlated with prefrontal activity and connectivity during emotion processing and had a significant association with SCZ negative symptom improvement, suggesting that miR-137–mediated coexpression may be implicated in clinical measures of SCZ, thus indicating a possible target for new SCZ treatments.

ACKNOWLEDGMENTS AND DISCLOSURES

This work was supported by the European Union Seventh Framework Programme for research, technological development, and demonstration (Grant No. 602450 [IMAGEMEND] [to AB]); by the European Union's Horizon 2020 research and innovation program under the Marie Skłodowska-Curie grant (Grant No. 798181 [to GP]); by European Union funding within the Ministero dell'Università e della Ricerca Piano Nazionale di Ripresa e Resilienza Extended Partnership initiative on Neuroscience and Neuropharmacology (Project No. PE00000006 CUP H93C22000660006 [to AB, GP, GB, and AR]); by the funding initiative Horizon Europe Seeds 2021 (Next Generation 8 European Union - Ministero dell'Università e della Ricerca Decreto Ministeriale 737/2021 for the project S68 CUP H99J21017550006 [to GP, AR, GB, and AB]); by the Apulian regional government (to AB); by the Canadian Institutes of Medical Research (Grant No. MOP-136916 [to JMB]); by the Fondazione Con Il Sud (to AB); by Exprivia SPA (to GP) under ministerial decree Decreto Ministeriale No. 352/22 and under a collaboration agreement (to AB); by the Consejo Nacional de Investigaciones Científicas y Técnicas, Argentina (to MNC); by Hoffmann-La Roche Ltd. (collaboration grant [to GP]) and through financial support (to ED and JD); by the 2021 Helmoltz Information and Data science Academy Grant (to RP and JD). JMB receives salary support as Canada Research Chair (Tier1) in Molecular Psychiatry. This paper reflects only the authors' views, and the European Union and Research Executive Agency are not liable for any use that may be made of the information contained herein. No funding body intervened in the manuscript preparation.

CommonMind Consortium data were generously provided to GP by the National Institute of Mental Health (NIMH) and CommonMind Consortium. Data were generated as part of the CommonMind Consortium supported by funding from Takeda Pharmaceuticals Company Limited, F. Hoffman-La Roche Ltd., and National Institutes of Health (Grant Nos. R01MH085542, R01MH093725, P50MH066392, P50MH080405, R01MH097276, R01MH075916, P50M096891, P50MH084053S1, R37MH057881, AG02219, AG05138, MH06692, R01MH110921, R01MH109677, R01MH109897, U01MH103392, and contract HHSN271201300031C) through the Division of Intramural Research Programs NIMH. Brain tissue for the study was obtained from the following brain bank collections: the Mount Sinai National Institutes of Health Brain and Tissue Repository, University of Pennsylvania Alzheimer's Disease Core Center, University of Pittsburgh NeuroBioBank and Brain and Tissue Repositories, and NIMH Human Brain Collection Core. CommonMind Consortium Leadership: Panos Roussos, Joseph Buxbaum, Andrew Chess, Schahram Akbarian, Vahram Haroutunian (Icahn School of Medicine at Mount Sinai), Bernie Devlin, David Lewis (University of Pittsburgh), Raquel Gur, Chang-Gyu Hahn (University of Pennsylvania), Enrico Domenici (University of Trento), Mette A. Peters, Solveig Sieberts (Sage Bionetworks), Thomas Lehner, Geetha Senthil, Stefano Marenco, Barbara K. Lipska (NIMH). UK Biobank Resource was used under approved project ID: 41655 in the Institute of Neuroscience and Medicine - INM-7: Brain and Behaviour at the Research Center Jülich (investigator, JD; collaborator, RP).

We thank Dr. Linda A. Antonucci, Dr. Barbara Gelao, Dr. Marina Mancini, Dr. Annamaria Porcelli, and Dr. Paolo Taurisano for data acquisition in Bari. We gratefully acknowledge the work by Prof. Roberto Bellotti and Dr. Sabina Tangaro (Department of Physics, University of Bari Aldo Moro), Dr. Lucia Colagiorgio, Dr. Anna Monda, and Elisabetta Volpe (former Department of Basic Medical Science, Neuroscience, and Sense Organs, University of Bari Aldo Moro), who contributed to data analysis. We also thank Prof. Simon Eickhoff (Research Center Jülich, Heinrich Heine University Düsseldorf) for providing access to UK Biobank data.

Gene expression data are available in public repositories. Neuroimaging and clinical data from the University of Bari Aldo Moro with demographic and behavioral characteristics cannot be shared at individual level in raw format because of ethic restrictions. UK Biobank neuroimaging data are available upon approved request (https://www.ukbiobank.ac.uk/). Summary statistics and code will be shared upon request.

AB received consulting fees from Biogen and lecture fees from Otsuka, Janssen, and Lundbeck. GB received lecture fees from Lundbeck. AR received travel fees from Lundbeck. MPap received travel fees from Newron Pharmaceuticals. ED was an employee of Hoffmann-La Roche Ltd. (2010–2015) and received research support from Hoffmann-La Roche Ltd. during the period 2016–2018. All other authors report no biomedical financial interests or potential conflicts of interest.

ARTICLE INFORMATION

From the Group of Psychiatric Neuroscience, Department of Translational Biomedicine and Neuroscience, University of Bari Aldo Moro, Bari, Italy (GP, AR, LS, CJB, RP, PDC, MNC, GCK, AL, MPap, TQ, RR, ST, HZ, GB, AB); Lieber Institute for Brain Development, Johns Hopkins Medical Campus, Baltimore, Maryland (GP, LS, CJB, GCK, MPar); Department of Psychiatry and Behavioral Sciences, Johns Hopkins University School of Medicine, Baltimore, Maryland (GP); Azienda Ospedaliero-Universitaria Consorziale Policlinico, Bari, Italy (AR, GB, AB); Institute of Neuroscience and Medicine, Brain & Behaviour, Research Centre Jülich, Jülich, Germany (RP, JD); Department of Pharmacology, University of Toronto, Toronto, Ontario, Canada (AMar, JK, JMB); Department of Medicine and Surgery, Libera Università Mediterranea Giuseppe Degennaro, Casamassima, Italy (LF); Dipartimento di Farmacia-Scienze del Farmaco, Università degli Studi di Bari Aldo Moro, Bari, Italy (NA); Istituto Nazionale di Fisica Nucleare, Sezione di Bari, Bari, Italy (NA, AMon); Consejo Nacional de Investigaciones Científicas y Técnicas, Ciudad Autónoma de Buenos Aires, Argentina (MNC); Grupo de Investigación en Neurociencias Aplicadas a las Alteraciones de la Conducta, Fleni-Consejo Nacional de Investigaciones Científicas y Técnicas Neurosciences Institute, Ciudad Autónoma de Buenos Aires, Argentina (MNC); Department of Cellular, Computational and Integrative Biology, University of Trento, Trento, Italy (ED); Fondazione The Microsoft Research University of Trento, Centre for Computational and Systems Biology, Rovereto, Italy (ED); Department of Molecular and Translational Medicine, University of Brescia, Brescia, Italy (MG, CM); Genetics Unit, Istituto di Ricovero e Cura a Carattere Sanitario Istituto Centro San Giovanni di Dio Fatebenefratelli, Brescia, Italy (MG); Department of Neuroscience, Novartis Institutes for Biomedical Research, Cambridge, Massachusetts (JK); Università degli Studi di Bari Aldo Moro, Dipartimento Interateneo di Fisica M. Merlin, Bari, Italy (AMon);

Istituto di Ricovero e Cura a Carattere Sanitario Istituto Centro San Giovanni di Dio Fatebenefratelli, Casa Sollievo della Sofferenza, San Giovanni Rotondo, Italy (TP); Department of Law, University of Foggia, Foggia, Italy (TQ); Department of Clinical and Experimental Sciences, University of Brescia, Brescia, Italy (PV); Department of Mental Health and Addiction Services, Azienda Socio Sanitaria Territoriale Spedali Civili of Brescia, Brescia, Italy (PV); and Institute of Systems Neuroscience, Medical Faculty, Heinrich Heine University Düsseldorf, Düsseldorf, Germany (JD).

GP and AR contributed equally to this work.

Address correspondence to Giulio Pergola, Ph.D., at giulio.pergola@uniba.it, or Antonio Rampino, M.D., Ph.D., at antonio.rampino@uniba.it.

Received Oct 31, 2022; revised Nov 4, 2023; accepted Nov 9, 2023.

Supplementary material cited in this article is available online at https://doi.org/10.1016/j.bpsc.2023.11.001.

REFERENCES

1. Sullivan PF, Kendler KS, Neale MC (2003): Schizophrenia as a complex trait: Evidence from a meta-analysis of twin studies. Arch Gen Psychiatry 60:1187–1192.
2. Parikshak NN, Gandal MJ, Geschwind DH (2015): Systems biology and gene networks in neurodevelopmental and neurodegenerative disorders. Nat Rev Genet 16:441–458.
3. Pergola G, Penzel N, Sportelli L, Bertolino A (2023): Lessons learned from parsing genetic risk for schizophrenia into biological pathways. Biol Psychiatry 94:121–130.
4. Trubetskoy V, Pardiñas AF, Qi T, Panagiotaropoulou G, Awasthi S, Bigdeli TB, *et al.* (2022): Mapping genomic loci implicates genes and synaptic biology in schizophrenia. Nature 604:502–508.
5. Cao H, Bertolino A, Walter H, Schneider M, Schäfer A, Taurisano P, *et al.* (2016): Altered functional subnetwork during emotional face processing: A potential intermediate phenotype for schizophrenia. JAMA Psychiatry 73:598–605.
6. Kauppi K, Westlye LT, Tesli M, Bettella F, Brandt CL, Mattingsdal M, *et al.* (2015): Polygenic risk for schizophrenia associated with working memory-related prefrontal brain activation in patients with schizophrenia and healthy controls. Schizophr Bull 41:736–743.
7. Krug A, Dietsche B, Zöllner R, Yüksel D, Nöthen MM, Forstner AJ, *et al.* (2018): Polygenic risk for schizophrenia affects working memory and its neural correlates in healthy subjects. Schizophr Res 197:315–320.
8. Miller JA, Scult MA, Conley ED, Chen Q, Weinberger DR, Hariri AR (2018): Effects of schizophrenia polygenic risk scores on brain activity and performance during working memory subprocesses in healthy young adults. Schizophr Bull 44:844–853.
9. Passiatore R, Antonucci LA, DeRamus TP, Fazio L, Stolfa G, Sportelli L, *et al.* (2023): Changes in patterns of age-related network connectivity are associated with risk for schizophrenia. Proc Natl Acad Sci USA 120:e2221533120.
10. Dzafic I, Burianová H, Periyasamy S, Mowry B (2018): Association between schizophrenia polygenic risk and neural correlates of emotion perception. Psychiatry Res Neuroimaging 276:33–40.
11. Erk S, Mohnke S, Ripke S, Lett TA, Veer IM, Wackerhagen C, *et al.* (2017): Functional neuroimaging effects of recently discovered genetic risk loci for schizophrenia and polygenic risk profile in five RDoC subdomains. Transl Psychiatry 7:e997.
12. Hauberg ME, Roussos P, Grove J, Børglum AD, Mattheisen M, Schizophrenia Working Group of the Psychiatric Genomics Consortium (2016): Analyzing the role of microRNAs in schizophrenia in the context of common genetic risk variants. JAMA Psychiatry 73:369–377.
13. Schizophrenia Working Group of the Psychiatric Genomics Consortium (2014): Biological insights from 108 schizophrenia-associated genetic loci. Nature 511:421–427.
14. Sakamoto K, Crowley JJ (2018): A comprehensive review of the genetic and biological evidence supports a role for MicroRNA-137 in the etiology of schizophrenia. Am J Med Genet B Neuropsychiatr Genet 177:242–256.
15. Guella I, Sequeira A, Rollins B, Morgan L, Torri F, van Erp TG, *et al.* (2013): Analysis of miR-137 expression and rs1625579 in dorsolateral prefrontal cortex. J Psychiatr Res 47:1215–1221.
16. Whalley HC, Papmeyer M, Romaniuk L, Sprooten E, Johnstone EC, Hall J, *et al.* (2012): Impact of a microRNA MIR137 susceptibility variant on brain function in people at high genetic risk of schizophrenia or bipolar disorder. Neuropsychopharmacology 37:2720–2729.
17. Mothersill O, Morris DW, Kelly S, Rose EJ, Fahey C, O'Brien C, *et al.* (2014): Effects of MIR137 on fronto-amygdala functional connectivity. Neuroimage 90:189–195.
18. Berboth S, Morawetz C (2021): Amygdala-prefrontal connectivity during emotion regulation: A meta-analysis of psychophysiological interactions. Neuropsychologia 153:107767.
19. Morawetz C, Bode S, Derntl B, Heekeren HR (2017): The effect of strategies, goals and stimulus material on the neural mechanisms of emotion regulation: A meta-analysis of fMRI studies. Neurosci Biobehav Rev 72:111–128.
20. Cosgrove D, Harold D, Mothersill O, Anney R, Hill MJ, Bray NJ, *et al.* (2017): MiR-137-derived polygenic risk: Effects on cognitive performance in patients with schizophrenia and controls. Transl Psychiatry 7:e1012.
21. Fazio L, Pergola G, Papalino M, Di Carlo P, Monda A, Gelao B, *et al.* (2018): Transcriptomic context of *DRD1* is associated with prefrontal activity and behavior during working memory. Proc Natl Acad Sci USA 115:5582–5587.
22. Pergola G, Di Carlo P, Jaffe AE, Papalino M, Chen Q, Hyde TM, *et al.* (2019): Prefrontal coexpression of schizophrenia risk genes is associated with treatment response in patients. Biol Psychiatry 86:45–55.
23. Antonucci LA, Di Carlo P, Passiatore R, Papalino M, Monda A, Amoroso N, *et al.* (2019): Thalamic connectivity measured with fMRI is associated with a polygenic index predicting thalamo-prefrontal gene co-expression. Brain Struct Funct 224:1331–1344.
24. Fromer M, Roussos P, Sieberts SK, Johnson JS, Kavanagh DH, Perumal TM, *et al.* (2016): Gene expression elucidates functional impact of polygenic risk for schizophrenia. Nat Neurosci 19:1442–1453.
25. Zhang B, Horvath S (2005): A general framework for weighted gene co-expression network analysis. Stat Appl Genet Mol Biol 4:Article17.
26. Trabzuni D, Ryten M, Walker R, Smith C, Imran S, Ramasamy A, *et al.* (2011): Quality control parameters on a large dataset of regionally dissected human control brains for whole genome expression studies. J Neurochem 119:275–282.
27. Pergola G, Di Carlo P, D'Ambrosio E, Gelao B, Fazio L, Papalino M, *et al.* (2017): DRD2 co-expression network and a related polygenic index predict imaging, behavioral and clinical phenotypes linked to schizophrenia. Transl Psychiatry 7:e1006.
28. GTEx Consortium (2015): Human genomics. The Genotype-Tissue Expression (GTEx) pilot analysis: Multitissue gene regulation in humans. Science 348:648–660.
29. Johnson MR, Shkura K, Langley SR, Delahaye-Duriez A, Srivastava P, Hill WD, *et al.* (2016): Systems genetics identifies a convergent gene network for cognition and neurodevelopmental disease. Nat Neurosci 19:223–232.
30. Langfelder P, Luo R, Oldham MC, Horvath S (2011): Is my network module preserved and reproducible? PLoS Comput Biol 7:e1001057.
31. Agarwal V, Bell GW, Nam JW, Bartel DP (2015): Predicting effective microRNA target sites in mammalian mRNAs. eLife 4:e05005.
32. Wong N, Wang X (2015): miRDB: An online resource for microRNA target prediction and functional annotations. Nucleic Acids Res 43:D146–D152.
33. Bandyopadhyay S, Mitra R (2009): TargetMiner: microRNA target prediction with systematic identification of tissue-specific negative examples. Bioinformatics 25:2625–2631.
34. Vlachos IS, Paraskevopoulou MD, Karagkouni D, Georgakilas G, Vergoulis T, Kanellos I, *et al.* (2015): DIANA-TarBase v7.0: Indexing more than half a million experimentally supported miRNA:mRNA interactions. Nucleic Acids Res 43:D153–D159.
35. Skene NG, Bryois J, Bakken TE, Breen G, Crowley JJ, Gaspar HA, *et al.* (2018): Genetic identification of brain cell types underlying schizophrenia. Nat Genet 50:825–833.
36. Gusev A, Mancuso N, Won H, Kousi M, Finucane HK, Reshef Y, *et al.* (2018): Transcriptome-wide association study of schizophrenia and chromatin activity yields mechanistic disease insights. Nat Genet 50:538–548.

37. Huckins LM, Dobbyn A, Ruderfer DM, Hoffman G, Wang W, Pardiñas AF, *et al.* (2019): Gene expression imputation across multiple brain regions provides insights into schizophrenia risk. Nat Genet 51:659–674.
38. Gandal MJ, Zhang P, Hadjimichael E, Walker RL, Chen C, Liu S, *et al.* (2018): Transcriptome-wide isoform-level dysregulation in ASD, schizophrenia, and bipolar disorder. Science 362:eaat8127.
39. Thomas PD, Campbell MJ, Kejariwal A, Mi H, Karlak B, Daverman R, *et al.* (2003): PANTHER: A library of protein families and subfamilies indexed by function. Genome Res 13:2129–2141.
40. Chen J, Bardes EE, Aronow BJ, Jegga AG (2009): ToppGene Suite for gene list enrichment analysis and candidate gene prioritization. Nucleic Acids Res 37:W305–W311.
41. Xu X, Wells AB, O'Brien DR, Nehorai A, Dougherty JD (2014): Cell type-specific expression analysis to identify putative cellular mechanisms for neurogenetic disorders. J Neurosci 34:1420–1431.
42. Chiang HR, Schoenfeld LW, Ruby JG, Auyeung VC, Spies N, Baek D, *et al.* (2010): Mammalian microRNAs: Experimental evaluation of novel and previously annotated genes. Genes Dev 24:992–1009.
43. Cheng Y, Wang ZM, Tan W, Wang X, Li Y, Bai B, *et al.* (2018): Partial loss of psychiatric risk gene Mir137 in mice causes repetitive behavior and impairs sociability and learning via increased Pde10a. Nat Neurosci 21:1689–1703.
44. Arakawa Y, Yokoyama K, Tasaki S, Kato J, Nakashima K, Takeyama M, *et al.* (2019): Transgenic mice overexpressing miR-137 in the brain show schizophrenia-associated behavioral deficits and transcriptome profiles. PLoS One 14:e0220389.
45. Pergola G, Di Carlo P, Andriola I, Gelao B, Torretta S, Attrotto MT, *et al.* (2016): Combined effect of genetic variants in the GluN2B coding gene (GRIN2B) on prefrontal function during working memory performance. Psychol Med 46:1135–1150.
46. D'Ambrosio E, Pergola G, Pardiñas AF, Dahoun T, Veronese M, Sportelli L, *et al.* (2022): A polygenic score indexing a DRD2-related co-expression network is associated with striatal dopamine function. Sci Rep 12:12610.
47. Braun U, Harneit A, Pergola G, Menara T, Schäfer A, Betzel RF, *et al.* (2021): Brain network dynamics during working memory are modulated by dopamine and diminished in schizophrenia. Nat Commun 12:3478.
48. Taurisano P, Pergola G, Monda A, Antonucci LA, Di Carlo P, Piarulli F, *et al.* (2021): The interaction between cannabis use and a CB1-related polygenic co-expression index modulates dorsolateral prefrontal activity during working memory processing. Brain Imaging Behav 15:288–299.
49. Selvaggi P, Pergola G, Gelao B, Di Carlo P, Nettis MA, Amico G, *et al.* (2019): Genetic variation of a DRD2 co-expression network is associated with changes in prefrontal function after D2 receptors stimulation. Cereb Cortex 29:1162–1173.
50. Rampino A, Walker RM, Torrance HS, Anderson SM, Fazio L, Di Giorgio A, *et al.* (2014): Expression of DISC1-interactome members correlates with cognitive phenotypes related to schizophrenia. PLoS One 9:e99892.
51. Alloza C, Blesa-Cábez M, Bastin ME, Madole JW, Buchanan CR, Janssen J, *et al.* (2020): Psychotic-like experiences, polygenic risk scores for schizophrenia, and structural properties of the salience, default mode, and central-executive networks in healthy participants from UK Biobank. Transl Psychiatry 10:122.
52. Rampino A, Taurisano P, Fanelli G, Attrotto M, Torretta S, Antonucci LA, *et al.* (2017): A Polygenic Risk Score of glutamatergic SNPs associated with schizophrenia predicts attentional behavior and related brain activity in healthy humans. Eur Neuropsychopharmacol 27:928–939.
53. Hagenaars SP, Harris SE, Davies G, Hill WD, Liewald DC, Ritchie SJ, *et al.* (2016): Shared genetic aetiology between cognitive functions and physical and mental health in UK Biobank (N=112 151) and 24 GWAS consortia. Mol Psychiatry 21:1624–1632.
54. Chen Q, Ursini G, Romer AL, Knodt AR, Mezeivtch K, Xiao E, *et al.* (2018): Schizophrenia polygenic risk score predicts mnemonic hippocampal activity. Brain 141:1218–1228.
55. Quarto T, Paparella I, De Tullio D, Viscanti G, Fazio L, Taurisano P, *et al.* (2018): Familial risk and a genome-wide supported DRD2 variant for schizophrenia predict lateral prefrontal-amygdala effective connectivity during emotion processing. Schizophr Bull 44:834–843.
56. Rampino A, Torretta S, Rizzo G, Viscanti G, Quarto T, Gelao B, *et al.* (2019): Emotional stability interacts with cortisol levels before fMRI on brain processing of fearful faces. Neuroscience 416:190–197.
57. Antonucci LA, Pergola G, Passiatore R, Taurisano P, Quarto T, Dispoto E, *et al.* (2020): The interaction between OXTR rs2268493 and perceived maternal care is associated with amygdala-dorsolateral prefrontal effective connectivity during explicit emotion processing. Eur Arch Psychiatry Clin Neurosci 270:553–565.
58. Callicott JH, Mattay VS, Bertolino A, Finn K, Coppola R, Frank JA, *et al.* (1999): Physiological characteristics of capacity constraints in working memory as revealed by functional MRI. Cereb Cortex 9:20–26.
59. Taurisano P, Antonucci LA, Fazio L, Rampino A, Romano R, Porcelli A, *et al.* (2016): Prefrontal activity during working memory is modulated by the interaction of variation in CB1 and COX2 coding genes and correlates with frequency of cannabis use. Cortex 81:231–238.
60. Lombardi A, Guaragnella C, Amoroso N, Monaco A, Fazio L, Taurisano P, *et al.* (2019): Modelling cognitive loads in schizophrenia by means of new functional dynamic indexes. NeuroImage 195:150–164.
61. Barch DM, Burgess GC, Harms MP, Petersen SE, Schlaggar BL, Corbetta M, *et al.* (2013): Function in the human connectome: Task-fMRI and individual differences in behavior. Neuroimage 80: 169–189.
62. Hariri AR, Tessitore A, Mattay VS, Fera F, Weinberger DR (2002): The amygdala response to emotional stimuli: A comparison of faces and scenes. Neuroimage 17:317–323.
63. Alfaro-Almagro F, Jenkinson M, Bangerter NK, Andersson JLR, Griffanti L, Douaud G, *et al.* (2018): Image processing and Quality Control for the first 10,000 brain imaging datasets from UK Biobank. Neuroimage 166:400–424.
64. Heinz A, Braus DF, Smolka MN, Wrase J, Puls I, Hermann D, *et al.* (2005): Amygdala-prefrontal coupling depends on a genetic variation of the serotonin transporter. Nat Neurosci 8:20–21.
65. Meyer JM, Nasrallah HA, McEvoy JP, Goff DC, Davis SM, Chakos M, *et al.* (2005): The Clinical Antipsychotic Trials Of Intervention Effectiveness (CATIE) Schizophrenia Trial: Clinical comparison of subgroups with and without the metabolic syndrome. Schizophr Res 80:9–18.
66. de Leeuw CA, Mooij JM, Heskes T, Posthuma D (2015): MAGMA: Generalized gene-set analysis of GWAS data. PLoS Comput Biol 11: e1004219.
67. Paus T, Keshavan M, Giedd JN (2008): Why do many psychiatric disorders emerge during adolescence? Nat Rev Neurosci 9:947–957.
68. Gogtay N, Vyas NS, Testa R, Wood SJ, Pantelis C (2011): Age of onset of schizophrenia: Perspectives from structural neuroimaging studies. Schizophr Bull 37:504–513.
69. Cabeza R, Nyberg L (2000): Imaging cognition II: An empirical review of 275 PET and fMRI studies. J Cogn Neurosci 12:1–47.
70. Kohler CG, Walker JB, Martin EA, Healey KM, Moberg PJ (2010): Facial emotion perception in schizophrenia: A meta-analytic review. Schizophr Bull 36:1009–1019.
71. Yamashita M, Yoshihara Y, Hashimoto R, Yahata N, Ichikawa N, Sakai Y, *et al.* (2018): A prediction model of working memory across health and psychiatric disease using whole-brain functional connectivity. eLife 7:e38844.
72. Gur RE, Calkins ME, Gur RC, Horan WP, Nuechterlein KH, Seidman LJ, Stone WS (2007): The Consortium on the Genetics of Schizophrenia: Neurocognitive endophenotypes. Schizophr Bull 33:49–68.
73. Park S, Gooding DC (2014): Working memory impairment as an endophenotypic marker of a schizophrenia diathesis. Schizophr Res Cogn 1:127–136.
74. Pergola G, Parihar M, Sportelli L, Bharadwaj R, Borcuk C, Radulescu E, *et al.* (2023): Consensus molecular environment of schizophrenia risk genes in coexpression networks shifting across age and brain regions. Sci Adv 9:eade2812.
75. Mahmoudi E, Cairns MJ (2017): MiR-137: An important player in neural development and neoplastic transformation. Mol Psychiatry 22:44–55.
76. Wray NR, Yang J, Hayes BJ, Price AL, Goddard ME, Visscher PM (2013): Pitfalls of predicting complex traits from SNPs. Nat Rev Genet 14:507–515.